

Probabilistic small-signal stability analysis of power system with solar farm integration

Samundra GURUNG*, Sumate NAETILADDANON^{ORCID}, Anawach SANGSWANG

Department of Electrical Engineering, Faculty of Engineering, King Mongkut's University of Technology Thonburi, Bangkok, Thailand

Received: 01.05.2018

Accepted/Published Online: 30.12.2018

Final Version: 22.03.2019

Abstract: Currently, large-scale solar farms are being rapidly integrated in electrical grids all over the world. However, the photovoltaic (PV) output power is highly intermittent in nature and can also be correlated with other solar farms located at different places. Moreover, the increasing PV penetration also results in large solar forecast error and its impact on power system stability should be estimated. The effects of these quantities on small-signal stability are difficult to quantify using deterministic techniques but can be conveniently estimated using probabilistic methods. For this purpose, the authors have developed a method of probabilistic analysis based on combined cumulant and Gram–Charlier expansion technique. The output from the proposed method provides the probability density function and cumulative density function of the real part of the critical eigenvalue, from which information concerning the stability of low-frequency oscillatory dynamics can be inferred. The proposed method gives accurate results in less computation time compared to conventional techniques. The test system is a large modified IEEE 16-machine, 68-bus system, which is a benchmark system to study low-frequency oscillatory dynamics in power systems. The results show that the PV power fluctuation has the potential to cause oscillatory instability. Furthermore, the system is more prone to small-signal instability when the PV farms are correlated as well as when large PV forecast error exists.

Key words: Cumulant method, forecast error, Gram–Charlier expansion, probability density function

1. Introduction

Recently, there has been a large proliferation of photovoltaic power generation (PVG) in electric power system and its aggregated production capacity is rapidly approaching the conventional generation capacity. Photovoltaic (PV) resources are highly attractive due to their inexhaustible availability in quantity and environmental friendliness. The total world PV generation reached 303 GW by the end of 2016 and will continue to grow as one of the most popular renewable sources. PV generation of 75 GW alone was added in the year 2016. However, PVG is highly intermittent and can severely degrade power quality and more dangerously power system stability [1].

There has been great effort in understanding the effect on probabilistic small-signal stability (PSSS). Broadly speaking, the current probabilistic method to analyze small-signal stability can be categorized into analytical and nonanalytical methods. The nonanalytical technique uses the Monte Carlo simulation (MCS) method to obtain information about system eigenvalue distribution [2]. This technique is based on a numerical method that requires running multiple deterministic small-signal stability analyses. As this method leads to a huge computational burden, many researchers only prefer it for the purpose of benchmarking.

*Correspondence: samundra24@gmail.com

The analytical methods employ complex mathematical approximations to infer the probability distribution of important electrical stability variables such as eigenvalues. A commonly used analytical method is the cumulant approach [3]. It has attracted large popularity and in-depth research because of its flexibility and computational efficiency [4]. The cumulant method is more accurate when compared with other analytical methods such as the point estimate method or probability collocation method [5]. This method is also widely used in PSSS [6–11]. More importantly, the effect of PV fluctuations on small-signal stability was studied in [10–18]. The authors in [10, 11] did extensive research on analyzing the impact of stochastic PV output on PSSS and observed that it can lead to a decrease in stability margin. The effect of combined PV and wind generation using MCS for a microgrid was studied in [12], where the authors concluded that fluctuations due to these two renewable sources have the potential to deteriorate small-signal stability. However, [10–12] were all based on small networks. The impact of small-signal stability is more severe on a large system as it can jeopardize system stability and ultimately lead to blackouts [13].

The impact of PVG on probabilistic low-frequency oscillatory stability using decision trees on a large transmission network was studied in [14]. The researchers in [15] investigated the effect of PV on dynamic stability on the IEEE-68 bus system using the cumulant method and concluded that the system can be stochastically unstable even when it is deterministically stable. In [16], a new method based on stochastic response surface was used to investigate the effect of PV uncertainties on a large system. The effect of different power system uncertainties including PVG on small-signal stability using game theory approach was studied in [17]. However, the methods proposed by the authors in [14, 17] require much computational time. Moreover, the papers discussed so far have not considered the possibility of correlation between solar farms. Different solar farms can be correlated due to insolation, temperature, and other environmental factors and can have detrimental effects on the system [1]. The effect of correlation between solar farms on PSSS was studied in [18] using copula theory and the authors found that correlation can lead to a decrease in system stability margin. However, the copula method is time-consuming and so computationally inefficient. Thus, there is a need to quantify the effect of correlation between PV farms on small-signal stability with an accurate and fast method.

Moreover, the growing penetration of renewable energy such as PV and wind has led to increased uncertainty, which results in significant error in renewable energy (RE) forecasting. This causes a large imbalance between electrical supply and demand and may lead to economic and reliability issues. Moreover, inaccuracy in forecast error can also lead to increased risk in system stability [9, 19].

Subsequently, there is a high need to fill the research gaps described here, especially in the current era of rapid large-scale integration of PVG, and to analyze its effect on small-signal stability of a large system using a fast yet accurate technique. This work is an augmented version of [15], where the study of effect of correlation between solar farms, impact of different penetration levels for various correlation coefficients, and effects of solar forecast error is added. The theory of cumulants considering correlated random variables is also added in our current work, which can be found in Section 5.3. Furthermore, we have also included a comparison between our proposed method with the technique developed by the authors of [10]. The main objectives and contributions of this paper are as follows:

- Development of a probabilistic model of PV output power using real measured data.
- Formulation of a framework to assess probabilistic small-signal stability in less computation time with highly accurate results considering stochastic PV output.
- Study of the impact of correlation between solar farms, solar forecast error, and change in penetration level on PSSS.

2. Framework of proposed methodology

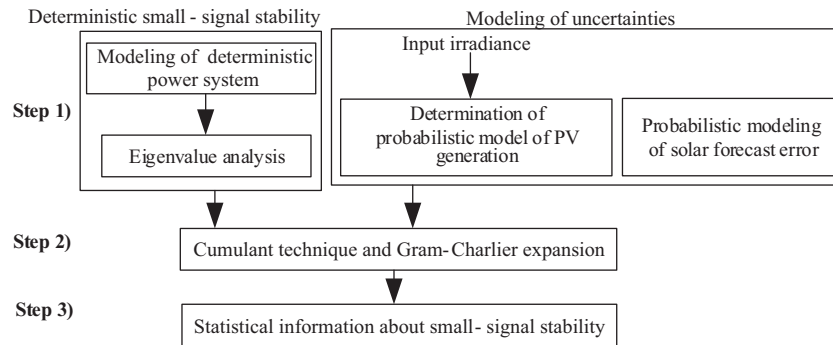


Figure 1. Proposed methodology to analyze probabilistic small-signal stability due to PV integration.

The proposed method to assess PSSS is shown in Figure 1 and can be stated as follows:

1. The first step involves running deterministic small-signal stability analysis. This process mainly comprises modeling of power system components and eigenvalue analysis, which are explained in Section 3.
2. The other major initial step requires modeling of uncertainty sources. The uncertainties are usually described by probability density function (PDF) or cumulative density function (CDF). This paper considers two uncertainties: one due to PV power fluctuations and another due to error in solar forecast, which are discussed in more detail in Section 4.
3. Once the deterministic power system and stochastic uncertainties are appropriately modeled, the combined method of cumulant and Gram–Charlier expansion is applied to obtain the statistical information about small-signal stability. More explanation of this step can be found in Section 5.

3. Deterministic small-signal stability

3.1. Modeling of deterministic power system

The power system consists of different components such as a synchronous generator, excitation system, and PV. All the synchronous generators are modeled using a sixth-order model and excitation systems are modeled as fast-acting IEEE ST1A type in this paper [20].

The PV model is developed as suggested by the North American Electric Reliability Corporation (NERC) and Western Electricity Coordinating Council (WECC) and is similar to the grid-side converter model of wind turbine generators (type 4 wind turbine generator) [21]. More details on PV converter and controller modeling can be found in [22, 23]. All the PV models are built using DIGSILENT in this paper.

3.2. Eigenvalue analysis

The power system's dynamic behavior can be represented with the following differential algebraic set of equations [20]:

$$\begin{aligned} \dot{x} &= f(x, y), \\ 0 &= g(x, y), \end{aligned} \quad (1)$$

where f is the vector of differential equations, x represents the vector of state variables, y is the vector of algebraic variables, and g is the vector of algebraic equations. The state matrix (A_S) can be obtained after linearizing and eliminating algebraic variables in Eq. (1) and thus it is implicitly assumed that the algebraic Jacobian matrix (g_y) is not singular (i.e. absence of singularity-induced bifurcation point) and is expressed as [13]:

$$A_S = f_x - f_y g_y^{-1} g_x, \quad (2)$$

where f_x, f_y, g_x , and g_y are the gradients computed at the operating point. Let the eigenvalue (λ) of Eq. (2) be

$$\lambda = -\sigma \pm j\omega, \quad (3)$$

where σ is the real part of the eigenvalue and ω is the imaginary part of the eigenvalue. The eigenvalues thus obtained from state matrix play a vital role in the field of deterministic small-signal stability analysis, as they exclusively determine the small-signal stability of the system. A system is said to be small-signal-stable if and only if all the real parts of the eigenvalues are negative. The imaginary part of the eigenvalue provides information about the frequency of the oscillation. As the real system can have hundreds of eigenvalues, only the critical eigenvalue (the eigenvalue whose real part is nearest to the origin) is used to analyze PSSS in this paper.

4. Modeling of uncertainties

4.1. Probabilistic modeling of PV fluctuation

4.1.1. Determination of probabilistic model of PV irradiance

The actual daily irradiance data collected from 2013 to 2016 by the CES Solar Cells Testing Center (CSSC), Thonburi, are used for analysis in this paper. The hourly data from 1200 to 1300 hours for the month of May are first used to construct the histogram for the purpose of fitting it to a distribution. This histogram is bimodal, with one peak lying on the lower irradiance and the other peak lying on the higher irradiance. However, only the histogram whose peak lies on higher irradiance is used here for fitting as it contains the majority of data, and no stability problem is found when the histogram with a peak lying on the low irradiance portion is considered during our analysis. The histogram of irradiance and the fitted distribution can be seen in Figure 2.

The histogram of irradiance best fits as a beta distribution, which can be seen from Table 1. Thus, the PDF of the solar irradiance can be written as [24]:

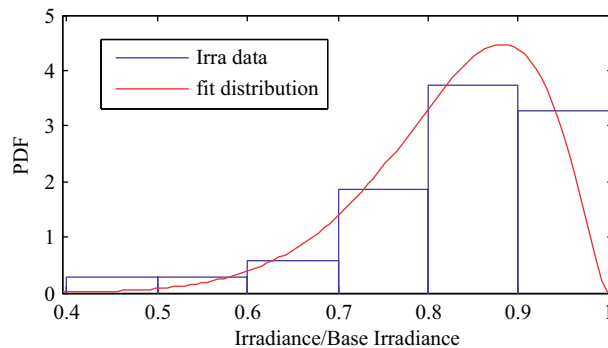


Figure 2. Distribution fit of solar irradiance.

Table 1. Parameters related to solar irradiance distribution.

Name	Value
Log likelihood	108.716
a	12.2101
b	2.48237
Mean (p.u)	0.831045
Variance	0.00894751
Base irradiance (W/m ²)	1100
ARMS (%)	0.242

$$f(S) = \frac{1}{B(a, b)} S^{a-1} (1 - S)^{b-1}, \quad (4)$$

where S is the irradiance, a and b are the shape parameters, and B is the beta function. The accuracy of the proposed probabilistic power model is calculated using the average root mean square (ARMS) [1]:

$$ARMS = \frac{\sqrt{\sum_{i=1}^N (F_{Mod,i} - F_{Ref,i})^2}}{N}, \quad (5)$$

where $F_{Mod,i}$ and $F_{Ref,i}$ are the i th values on the CDF curves of the fitted model and the reference model, respectively, and N is the selected number of points. The ARMS for this case is 0.242%, showing the validity of the proposed probabilistic model.

4.1.2. Probabilistic modeling of PV output power

The power output of PVG varies linearly with the irradiance and is given by [25]:

$$P_i = \left(\frac{S}{S_{base}} \right) P_{rated}, \quad (6)$$

where P_i is the power injection for the i th PV, P_{rated} is the rated PV output power, S is the actual irradiance (W/m²), and S_{base} is the base irradiance. The PDF of PVG for the i th farm (f_{p_i}) can be obtained by substituting Eq. (4) in Eq. (6) and then using the well-known transformation method [19]:

$$f_{p_i}(P_i) = \frac{1}{P_{rated}} \frac{1}{B(a, b)} \left(\frac{P_i}{P_{rated}} \right)^{a-1} \left(1 - \frac{P_i}{P_{rated}} \right)^{b-1}, \text{ for } 0 < P_i < P_{max}, \quad (7)$$

where P_{max} is the maximum output power.

4.2. Modeling of solar forecast error

Forecast error varies widely with the hour of the day as well as the feeding power. The PV forecast error is normally modeled as a Gaussian distribution and the expression for the PDF of the i th PV farm output is given by [26, 27]:

$$f(X_{P_i}) = \frac{1}{\sigma\sqrt{2\pi}} \exp\left(-\frac{[X_{P_i} - (X_{P_{i_0}} + \mu)]^2}{2\sigma^2}\right), \quad (8)$$

where X_{P_i} is the actual output of the i th PV farm; $X_{P_{i_0}}$ is the forecast value of the i th PV farm, which is deterministic; and μ and σ are the mean and standard deviation of PV forecast error, respectively.

5. Proposed method to solve PSSS

The proposed method uses a combined cumulant and Gram–Charlier expansion technique to solve the PSSS.

5.1. Calculation of input cumulants

The PV power variation is defined as $\Delta P_i = P_i - P_d$, where P_i is the active power supplied by the i th PV farm and P_d is the deterministic PV power generation. The n th raw moment of the PV power variation ($\alpha_{\Delta P_i}^{(n)}$) can be computed as follows [24]:

$$\begin{aligned} \alpha_{\Delta P_i}^{(n)} &= \int_0^{P_{rated}} x^n f_{p_i}(x) dx \\ &= \frac{1}{B(a, b)} \int_0^{P_{rated}} x^n \times (x + P_i)^{a-1} [1 - (x + P_i)]^{b-1} dx. \end{aligned} \tag{9}$$

Let $t = x + P_i$. Then $dt = dx$, and then Eq. (9) becomes:

$$\begin{aligned} \alpha_{\Delta P_i}^{(v)} &= \frac{1}{B(a, b)} \int_0^1 (t - P_i)^n \times t^{a-1} \times (1 - t)^{b-1} dt \\ &= \frac{1}{B(a, b)} \sum_{k=0}^n C_k^n \int_0^1 t^k (-P_i)^{n-k} \times t^{a-1} (1 - t)^{b-1} dt \\ &= \sum_{k=0}^n C_k^n \frac{(-P_i)^{n-k}}{B(a, b)} \int_0^1 t^{(a+k)-1} \times (1 - t)^{b-1} dt \\ &= \sum_{k=0}^n C_k^n (-P_i)^{n-k} \times \frac{B(a + k, b)}{B(a, b)}, \end{aligned} \tag{10}$$

where $C_n^k = n!/(k!(n - k)!)$, $B(a + k, b) = \Gamma(a + k)\Gamma(b)/\Gamma(a + b + k)$, and Γ is the gamma function. Eq. (10) provides a very simple analytical solution for input power deviation of a solar farm and can be used in other probabilistic methods based on the cumulant method to analyze different aspects of power systems such as probabilistic load-flow, reliability assessment, or stability, which contains the PVG with beta distribution in the test system. Similarly, the raw moments when forecast error is considered can be computed as:

$$\alpha_{\Delta P_i}^{(n)} = \int_{-\infty}^{\infty} x^n f(x) dx. \tag{11}$$

The v th order cumulants of input power fluctuation ($K_{\Delta P_i}^{(v)}$) can be calculated as follows [1]:

$$\begin{aligned} K_{\Delta P_i}^{(1)} &= \alpha_{\Delta P_i}^{(1)}, \\ K_{\Delta P_i}^{(2)} &= \alpha_{\Delta P_i}^{(2)} - \alpha_{\Delta P_i}^{(1)}, \\ K_{\Delta P_i}^{(3)} &= \alpha_{\Delta P_i}^{(3)} - 3\alpha_{\Delta P_i}^{(1)}\alpha_{\Delta P_i}^{(2)} + 2\left(\alpha_{\Delta P_i}^{(1)}\right)^3, \\ &\dots \end{aligned} \tag{12}$$

5.2. Linearization and sensitivity calculation

Assuming there are N PV systems in the power system and $\lambda_k = \sigma_k + j\omega_k$, which denotes the k th eigenvalue (critical) of the power system with real part (σ_k) and imaginary part (ω_k), the following relationship can be established after linearization [28]:

$$\Delta\lambda_k = \Delta\sigma_k + j\Delta\omega_k = \sum_{i=1}^N \frac{\partial\lambda_k}{\partial P_i} \Delta P_i, \quad (13)$$

$$\frac{\partial\lambda_k}{\partial P_i} = \frac{\lambda_k(P_i + \Delta P_i) - \lambda_k(P_i)}{\Delta P_i}. \quad (14)$$

The sensitivity term of Eq. (14) can be derived either analytically or numerically. It is calculated numerically here as it is much simpler and still gives high accuracy results [28].

5.3. Calculation of output cumulants

The self cumulants for the first and second order of the critical eigenvalue (output) can be written as [29]:

$$\begin{aligned} K_{\Delta\sigma_k}^{(1)} &= \sum_{i=1}^N \operatorname{Re} \left(\frac{\partial\lambda_k}{\partial P_i} \right) \mu_{\Delta P_i}, \\ K_{\Delta\sigma_k}^{(2)} &= \sum_{i=1}^N \operatorname{Re} \left(\frac{\partial\lambda_k}{\partial P_i} \right)^2 + 2 \sum_{i=1, i < j}^N \operatorname{Re} \left(\frac{\partial\lambda_k}{\partial P_i} \right) \operatorname{Re} \left(\frac{\partial\lambda_k}{\partial P_j} \right) K_{\Delta P_i, \Delta P_j}, \\ &\dots \end{aligned} \quad (15)$$

More importantly, $K_{\Delta P_i, \Delta P_j} = \sigma_{\Delta P_i}^2$, $K_{\Delta P_i, \Delta P_j} = \operatorname{cov}(\Delta P_i, \Delta P_j) = \rho \Delta P_i \Delta P_j$, where ρ is the correlation coefficient between two random variables ΔP_i and ΔP_j and $\sigma_{\Delta P_i}$ is the standard deviation of power fluctuation for the i th PV farm. If $\Delta P_1, \Delta P_2, \dots, \Delta P_n$ are independent, the v th order output cumulant ($K_{\Delta\sigma_k}^{(v)}$) is given by [3]:

$$K_{\Delta\sigma_k}^{(v)} = \sum_{i=1}^N \left[\operatorname{Re} \left(\frac{\partial\lambda_k}{\partial P_i} \right) \right]^v K_{\Delta P_i}^{(v)}. \quad (16)$$

5.4. Gram–Charlier expansion to find PDF and CDF of the output variable

When the output cumulants are calculated, the PDF and CDF of the critical eigenvalue can be constructed with the help of Gram-Charlier expansion [3]. Unlike other expansion techniques such as Edgeworth expansion, Cornish–Fisher expansion, etc., this expansion method does not show error in the tail regions [1] and is widely used in the field of PSSS [6–8, 10, 11].

5.5. Calculation of stability index

Finally, the probability of instability (PIS) is calculated [6] as:

$$\begin{aligned} F_{\sigma_k}(0) &= P(\sigma_k \leq 0) = \int_{-\infty}^0 f_{\sigma_k}(x) dx, \\ PIS &= 1 - F_{\sigma_k}(0), \end{aligned} \quad (17)$$

where F_{σ_k} is the CDF of the real part of the critical eigenvalue and f_{σ_k} is the PDF of the real part of the critical eigenvalue. The PIS gives the probability of the real part of the critical eigenvalue being greater than zero or alternatively provides the information about the probability of the power system being small-signal-unstable.

5.6. Summary of PM to assess PSSS

The algorithm developed to assess PSSS can be summarized as:

1. Probabilistic modeling of PV fluctuation and solar forecast error by applying Eqs. (7) and (8), respectively.
2. The probabilistic models are then used to find the input moments by using Eq. (10) or Eq. (11) depending on the input uncertainty. This is a crucial part as the expression for the input moment needs to be derived and is unique for each uncertainty.
3. Calculation of sensitivity factor by applying Eq. (14).
4. The output cumulants are then found by using Eq. (15) for correlated and Eq. (16) for uncorrelated cases.
5. Finally, Eq. (17) is used to calculate the PIS, which provides information about small-signal stability.

6. Results and discussion

6.1. Test system

Figure 3 shows the test system, which has 16 machines and 5 areas and is a reduced order equivalent to the interconnected New England Test System (NETS) and New York Power System (NYPS). As the location of PV farms is not the primary concern in our research, it is assumed that three PV farms are each connected at buses 18, 41, and 42. All the PV generators are rated at 100 MVA with unity power factor but are assumed to operate at 0.83 p.u. (83 MW). A power oscillation damping controller and power system stabilizer are occasionally used to improve small-signal stability for the test system considered in our work [15, 20]. However, we have not used these controllers for our current study as we want this paper to focus exclusively on comprehensive quantification of the effect of uncertainties due to solar energy under different conditions on small-signal stability. Thus, all power system stabilizers are assumed to be disabled in our study. The parameters of excitation systems and generators are taken from [20].

6.2. Analysis of case studies

6.2.1. PV penetration in uncorrelated case

In the first case, the PV farms located at three places in the test system are assumed to be uncorrelated. All the case studies in this paper are computed using Intel Core i5-2400 CPU, 3.17 GHz processing speed with 8 GB RAM. The comparison between the results obtained from the proposed method and MCS method (obtained with 10,000 simulations) is shown in Table 2. The method proposed in [10] is also applied for comparison with our proposed method. The important statistical parameters such as mean and standard deviation (Std) along with PIS and the computation time are compared. The output from PM and MCS matches very closely as ARMS is a mere 0.1416%. Furthermore, it can be seen that the compared method of [10] overestimates the value for PIS, validating the higher accuracy of our technique. The PDF of the real part of the critical eigenvalue is shown in Figure 4, which clearly has some part of its area lying on the positive half plane. Figure 5 shows the

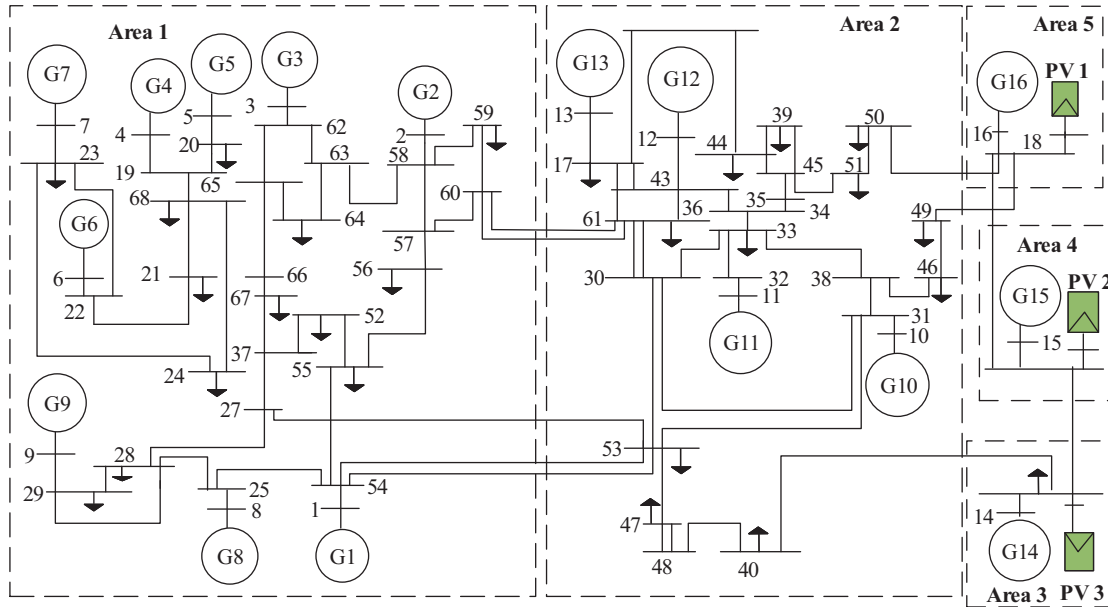


Figure 3. Modified IEEE 68-bus system.

CDF of the real part of the critical eigenvalue. This suggests that the given test system has a chance of being small-signal-unstable, which is also confirmed from the PIS value of 18.04%.

Table 2. Comparison of results for real part of critical eigenvalue.

	MCS	PM	Reference [10]
ARMS (%)	-	0.1416	-
Mean	-0.0002863	-0.00028431	-0.00028365
Std	0.000313292	0.000318756	0.000335977
PIS (%)	18.04	19.32	20.7682
Time (s)	4553.46	40.8	41.22

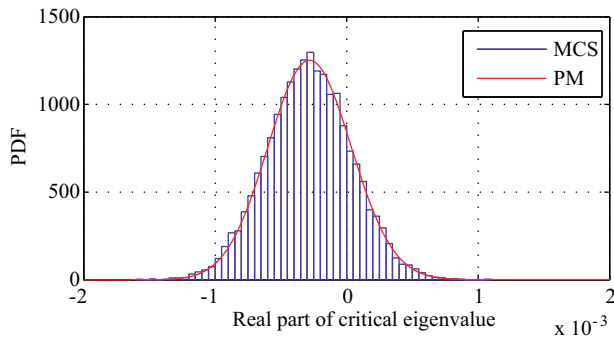


Figure 4. PDF of the real part of critical eigenvalue.

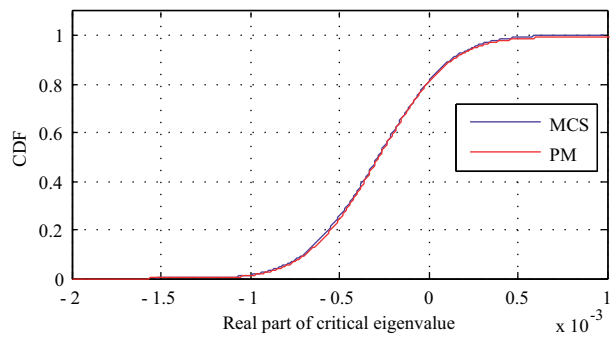


Figure 5. CDF of the real part of critical eigenvalue.

6.2.2. Analysis during correlated condition

The second case deals with the condition when the PV farms located at three different locations are assumed to be correlated. The correlation coefficient between PV farms is taken as 0.8 [30]. In this case, correlated random numbers need to be generated while applying the MCS method. This paper uses the Gaussian copula method for this purpose [31]. As can be seen from Table 3, the two methods relate closely, with ARMS of only 0.1486%. The computation time for PM is also 110.71 times faster than MCS. The correlation effect pushes PIS to 23.723%, which is around 5.683% higher compared to the previous case. Additionally, it can be seen from Table 3 that the method proposed in [10] underestimates the value of PIS. Figures 6 and 7 show the PDF and CDF of the real part of the critical eigenvalue in the correlated case. As can be seen from Figure 6, the spread of the PDF in the correlated case is much higher than in the uncorrelated case.

Table 3. Comparison of results for real part of critical eigenvalue in correlated case.

	MCS	PM	Reference [10]
ARMS (%)	-	0.1486	-
Mean	-0.00027651	-0.0002843172	-0.000309873
Std	0.000385389	0.000388465	0.000395023
PIS (%)	23.723	23.13	21.6390
Time (s)	4705.3	42.5	43.33

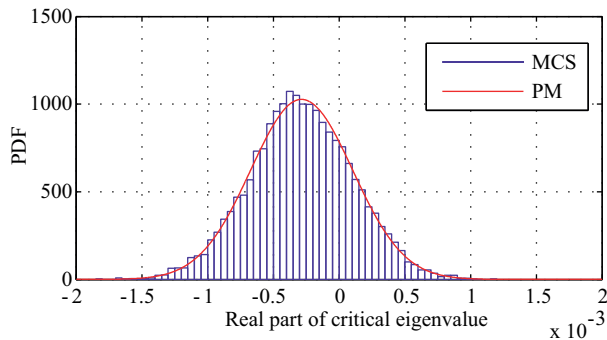


Figure 6. PDF of the real part of critical eigenvalue in correlated case.

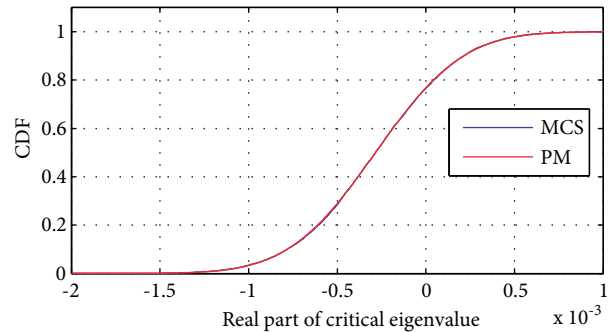


Figure 7. CDF of the real part of critical eigenvalue in correlated case.

Table 4. Comparison of results for real part of critical eigenvalue for different correlated coefficients.

	Corr. coeff.=0.8	Corr. coeff.=0.85	Corr. coeff.=0.9	Corr. coeff.=0.95	Corr. coeff.=1.0
Mean	-0.000284312	-0.000284312	-0.000284312	-0.000284312	-0.000284312
Std	0.000388465	0.00039241	0.00039631749	0.0004040172	0.000404017297
PIS (%)	23.13	23.43708	23.58	24	24.0805

According to Table 4 and Figure 8, the PIS along with the standard deviation of the critical eigenvalue increases by a very small amount with the increase in correlation coefficient.

6.2.3. Impact of solar forecast error

The forecast value for all the PV farms is taken as 0.831 p.u. The standard deviation of forecast error (σ) is taken as 20% of the forecast value. The PDF of solar forecast error is shown in Figure 9.

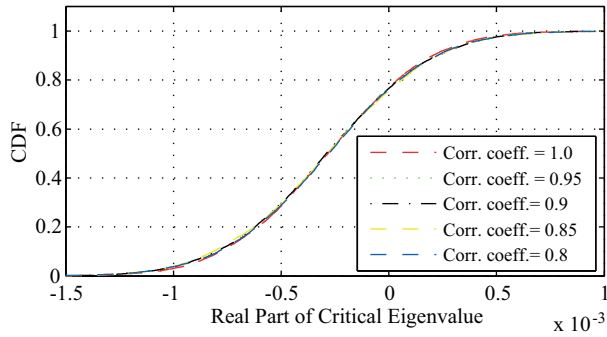


Figure 8. CDF for different correlation coefficients.

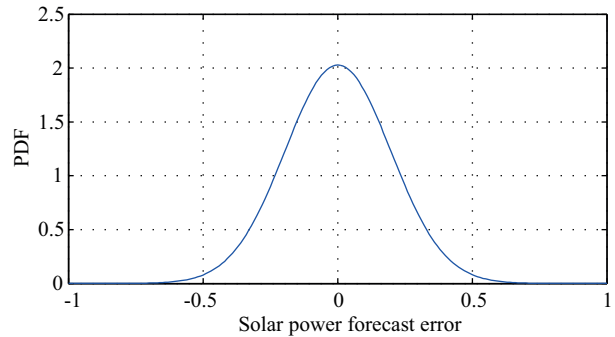


Figure 9. Probability distribution of solar forecast error.

The PDF and CDF of the real part of the critical eigenvalue due to forecast error is shown in Figure 10 and Figure 11, respectively. The PIS as a result of forecast error is found to be 30.73%.

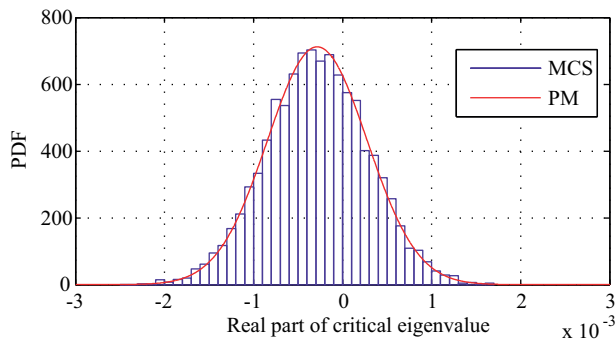


Figure 10. PDF of the real part of critical eigenvalue due to solar forecast error.

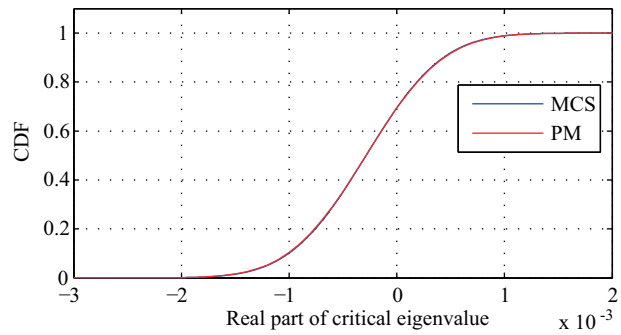


Figure 11. CDF of the real part of critical eigenvalue due to solar forecast error.

According to the results in Table 5, the outputs from both methods match closely with ARMS of less than 1%. Furthermore, the method proposed in [10] and PM both provide accurate estimation of the value of PIS for this case.

Table 6 shows the results for different percentage values of standard deviation of forecast error for the same forecast value (0.831 p.u.). The results depict that large forecast error leads to an increase in deterioration of small-signal stability.

6.2.4. Increase in PV penetration

This case analyzes the impact of change in PV rating on PSSS, where the change is calculated with respect to its base value (100 MVA). Thus, a 10% increase refers to the condition when all the PV farms are operating at 0.1 p.u. (10 MVA). The same values of shape parameters are used for the PDF of PV output power, which are provided in Section 4.1.1, for this case study. Moreover, this case also analyzes PV penetration under different correlation coefficients. According to Figure 12, PIS increases with the increase in penetration rating of PVG.

Table 5. Comparison of results for real part of critical eigenvalue considering solar forecast error.

	MCS	PM	Reference [10]
ARMS (%)	-	0.1395	-
Mean	-0.00028572	-0.000284311	-0.00028325
Std	0.00056756	0.000560121	0.00055311
PIS (%)	30.7335	30.587	30.4289
Time (s)	4689.64	39.5	43.33

Table 6. Comparison of results for real part of critical eigenvalue for different forecast error deviations.

	$\sigma = 10\%$	$\sigma = 20\%$	$\sigma = 30\%$	$\sigma = 40\%$	$\sigma = 50\%$
Mean	-0.000284311	-0.000284311	-0.000284311	-0.000284311	0.000284311
Std	0.00027995	0.000560121	0.00083986	0.00111981	0.00139977
PIS (%)	15.408	30.587	36.7046	39.945	41.925

This condition is always more severe in correlated condition and is highest when the correlation coefficient equals 1.0 compared to uncorrelated condition.

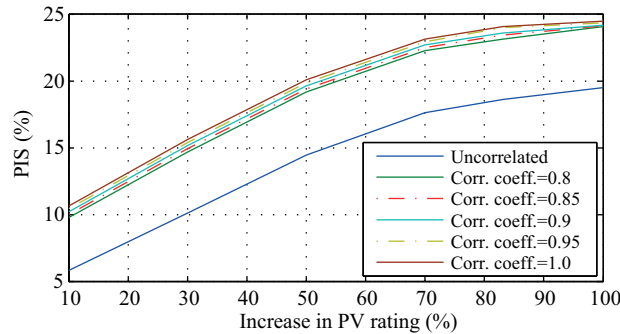


Figure 12. Probability of instability in percentage for different penetration levels.

7. Conclusions

In this paper, the proposed probabilistic method is applied to analyze the effect of PV uncertainties arising mainly due to stochastic PV fluctuations and forecast error on small-signal stability. The developed framework can provide accurate results to assess PSSS in much less computation time compared to conventional MCS and other analytical techniques. We observed that the fluctuation due to PVG results in the given test system being stochastically unstable. Furthermore, the probability of the system being small-signal-stable reduces with the increase in correlation coefficient between solar farms and is lowest when the value of coefficient is 1. It is also seen that the increase in deviation of forecast error greatly reduces PSSS. Finally, the increase in PV penetration increases the value of PIS for the given test system.

This research work can be highly useful for system planners for decision-making as it provides much more information about system stability compared to the deterministic method. Our future works will involve designing efficient damping controllers by directly considering the stochastic fluctuations due to PVG and investigation of potential use of battery energy storage systems to improve PSSS.

Acknowledgment

The authors would like to thank the Petchra Pra Jom Klao research scholarship funded by King Mongkut's University of Technology Thonburi for support.

References

- [1] Fan M, Vittal V, Heydt GT, Ayyanar R. Probabilistic power flow studies for transmission systems with photovoltaic generation using cumulants. *IEEE Transactions on Power Systems* 2012; 27 (4): 2251-2261.
- [2] Xu Z, Dong ZY, Zhang P. Probabilistic small signal analysis using Monte Carlo simulation. In: *IEEE 2005 Power Engineering Society General Meeting*; San Francisco, CA, USA; 2005. pp. 1658-1664.
- [3] Zhang P, Lee ST. Probabilistic load flow computation using the method of combined cumulants and Gram-Charlier expansion. *IEEE Transactions on Power Systems* 2004; 19 (1): 676-682.
- [4] Xifan W, Yonghua S, Malcolm I. *Modern Power System Analysis*. New York, NY, USA: Springer, 2008.
- [5] Preece R, Huang K, Milanović JV. Probabilistic small-disturbance stability assessment of uncertain power systems using efficient estimation methods. *IEEE Transactions on Power Systems* 2014; 29 (5): 2509-2517.
- [6] Bu SQ, Du W, Wang HF, Chen Z, Xiao LY et al. Probabilistic analysis of small-signal stability of large-scale power systems as affected by penetration of wind generation. *IEEE Transactions on Power Systems* 2012; 27 (2): 762-770.
- [7] Bu SQ, Du W, Wang HF. Probabilistic analysis of small-signal rotor angle/voltage stability of large-scale AC/DC power systems as affected by grid-connected offshore wind generation. *IEEE Transactions on Power Systems* 2013; 28 (4): 3712-3719.
- [8] Bu SQ, Du W, Wang HF. Investigation on probabilistic small-signal stability of power systems as affected by offshore wind generation. *IEEE Transactions on Power Systems* 2015; 30 (5): 2479-2486.
- [9] Wang ZW, Shen C, Liu F. Probabilistic analysis of small signal stability for power systems with high penetration of wind generation. *IEEE Transactions on Sustainable Energy* 2016; 7 (3): 1182-1193.
- [10] Liu S, Liu PX, Wang X. Stochastic small-signal stability analysis of grid-connected photovoltaic systems. *IEEE Transactions on Industrial Electronics* 2016; 63 (2): 1027-1038.
- [11] Liu S, Liu PX, Wang X. Stability analysis of grid-interfacing inverter control in distribution systems with multiple photovoltaic-based distributed generators. *IEEE Transactions on Industrial Electronics* 2016; 63 (12): 7339-7348.
- [12] Krismanto AU, Mithulananthan N, Kamwa I. Oscillatory stability assessment of microgrid in autonomous operation with uncertainties. *IET Renewable Power Generation* 2017; 12 (4): 494-504.
- [13] Prasertwong K, Mithulananthan N, Thakur D. Understanding low-frequency oscillation in power systems. *International Journal of Electrical Engineering & Education* 2010; 47 (3): 248-262.
- [14] Wang T, Bi T, Wang H, Liu J. Decision tree based online stability assessment scheme for power systems with renewable generations. *CSEE Journal of Power and Energy Systems* 2015; 1 (2): 53-61.
- [15] Gurung S, Naetiladdan S, Sangswang A. Impact of photovoltaic penetration on small signal stability considering uncertainties. In: *Innovative Smart Grid Technologies-Asia*; Auckland, New Zealand; 2017. pp. 1-6.
- [16] Zhou Y, Li Y, Liu W, Yu D, Li Z et al. The stochastic response surface method for small-signal stability study of power system with probabilistic uncertainties in correlated photovoltaic and loads. *IEEE Transactions on Power Systems* 2017; 32 (6): 4551-4559.
- [17] Hasan KN, Preece R, Milanovic J. Application of game theoretic approaches for identification of critical parameters affecting power system small-disturbance stability. *International Journal of Electrical Power & Energy Systems* 2018; 97: 344-352.

- [18] Hasan KN, Preece R. Influence of stochastic dependence on small-disturbance stability and ranking uncertainties. *IEEE Transactions on Power Systems* 2018; 33 (3): 3227-3235.
- [19] Preece R, Milanović JV. Risk-based small-disturbance security assessment of power systems. *IEEE Transactions on Power Delivery* 2015; 30 (2): 1-9.
- [20] Pal B, Chaudhuri B. *Robust Control in Power Systems*. New York, NY, USA: Springer, 2005.
- [21] Tamimi B, Cañizares C, Bhattacharya K. System stability impact of large-scale and distributed solar photovoltaic generation: the case of Ontario, Canada. *IEEE Transactions on Sustainable Energy* 2013; 4 (3): 680-688.
- [22] Fortmann J, Engelhardt S, Kretschmann J, Feltes C, Erlich I. New generic model of DFIG-based wind turbines for RMS-type simulation. *IEEE Transactions on Energy Conversion* 2014; 29 (1): 110-118.
- [23] Erlich I, Shewarega F, Feltes C, Koch F, Fortmann J. Determination of dynamic wind farm equivalents using heuristic optimization. In: *IEEE 2012 Power and Energy Society General Meeting*; San Diego, CA, USA; 2012. pp. 1-8.
- [24] Bertsekas DP, Tsitsiklis JN. *Introduction to Probability*. Belmont, MA, USA: Athena Scientific, 2002.
- [25] Aien M, Fotuhi-Firuzabad M, Rashidinejad M. Probabilistic optimal power flow in correlated hybrid wind-photovoltaic power systems. *IEEE Transactions on Smart Grid* 2014; 5 (1): 130-138.
- [26] Breuer C, Engelhardt C, Moser A. Expectation-based reserve capacity dimensioning in power systems with an increasing intermittent feed-in. In: *IEEE 2013 European Energy Market (EEM)*; Stockholm, Sweden; 2013. pp. 1-7.
- [27] Agalgaonkar YP, Pal BC, Jabr RA. Stochastic distribution system operation considering voltage regulation risks in the presence of PV generation. *IEEE Transactions on Sustainable Energy* 2015; 6 (4): 1315-1324.
- [28] Dong ZY, Pang CK, Zhang P. Power system sensitivity analysis for probabilistic small signal stability assessment in a deregulated environment. *International Journal of Control Automation and Systems* 2005; 3 (2): 355-362.
- [29] McCullagh P. *Tensor Methods in Statistics*. New York, NY, USA: Chapman and Hill, 1987.
- [30] Widén J. Correlations between large-scale solar and wind power in a future scenario for Sweden. *IEEE Transactions on Sustainable Energy* 2011; 2 (2): 177-184.
- [31] Papaefthymiou G, Kurowicka D. Using copulas for modeling stochastic dependence in power system uncertainty analysis. *IEEE Transactions on Power Systems* 2009; 24 (1): 40-49.